Killowatt-peak-power, single-frequency, pulsed fiber laser near 2 μm

Jihong Geng,[1,*] Qing Wang,[1] Zack Jiang,[1] Tao Luo,[1] Shibin Jiang,[1] and Gregory Czarnecki[2]

[1]*AdValue Photonics, 3708 East Columbia Street, Suite 100, Tucson, Arizona 85714, USA*

[2]*Wright-Patterson Air Force Base, 46th Test Wing, Ohio 45433-7605, USA*

**Corresponding author: jgeng@advaluephotonics.com*

Received April 19, 2011; revised May 18, 2011; accepted May 19, 2011;
posted May 19, 2011 (Doc. ID 146192); published June 13, 2011

We generated single-frequency pulses at kilowatt peak power from an all-fiber Tm-doped master oscillator power amplifier system, which is the first report of this kind (to the best of our knowledge) of a laser in the 2 μm region. Compared with the laser linewidth of seed pulses, spectral broadening by a factor of 3 was observed with the amplified pulses. This was attributed to self-phase modulation in passive pigtail fibers of the components (isolator and wavelength division multiplexing) that were placed after the fiber amplifier. The short pulse width (~7 ns) of the kilowatt-level pulses prevents an onset of stimulated Brillouin scattering in the long fiber. When launching the pulses into several-meter single-mode fiber, significant nonlinear spectral broadening occurs due to modulation instability in the fiber. This reaction is beneficial for generation of a mid- and long-wavelength IR supercontinuum in nonlinear IR fibers. © 2011 Optical Society of America

OCIS codes: 060.2320, 140.3540, 140.3510, 140.3570.

High-power, single-frequency pulsed lasers operating in the spectral region near 2 μm are highly desirable for many applications, including airborne and spaceborne coherent lidar for atmospheric sensing [1–4] and nonlinear frequency conversion for the generation of narrowband mid-IR radiation [5,6]. Such lasers can also be used as pump sources for mid- and long-wavelength broadband supercontinuum generation [7]. Although high-power pulsed single-frequency Tm- or Ho-doped crystal lasers were demonstrated decades ago, they suffer from a complicated free-space laser cavity design with the concern of long-term reliability. Fiber-based laser sources are much more reliable and more suitable for these applications, especially for field deployment.

Recently, we demonstrated the first all-fiber, *Q*-switched, single-frequency laser oscillator near 2 μm [8]. In this Letter, we report the generation of kilowatt-level single-frequency laser pulses from an all-fiber Tm-doped source. Similar fiber-based single-frequency pulses operating at 1.55 μm have been reported recently [9], but this is, to our best knowledge, the first demonstration of this kind of laser in the 2 μm region. Short pulses (~7 ns) from the laser oscillator and the short length of active fiber used in the fiber amplifier prevent the onset of stimulated Brillouin scattering (SBS), which is usually the major limiting factor in high-power single-frequency fiber sources. As compared to the seed pulses, amplified single-frequency pulses exhibit a slightly broadened spectral linewidth by a factor of 3, due to their high peak power. This spectral broadening was attributed to self-phase modulation (SPM) induced by the meters-long passive fibers of an isolator and wavelength division multiplexing (WDM), rather than the short active fiber in the fiber amplifier. Furthermore, after launching pulses into a long passive single-mode fiber, significant spectral broadening can be induced by modulation instability (MI, or four-wave mixing), which is beneficial to further generate mid- and long-wavelength IR supercontinuum in nonlinear IR fibers [7].

Figure 1 shows the experimental setup. The kilowatt single-frequency pulsed Tm-doped fiber laser was pumped by a single Er-doped fiber source at 1.55 μm. A small part (~30%) of the Er-fiber laser was split out to pump the laser oscillator, generating several to tens of milliwatts of average power of single-frequency pulses at 1950 nm. The single-frequency operation was confirmed by using a scanning fiber Fabry–Perot interferometer (800 MHz free spectral range and ~8 MHz spectral resolution) that was built in-house and described in our previous work [8]. Figure 2 shows average output power as a function of the pulse repetition rate at a pump power of 300 mW. The laser pulse duration is dependent on both repetition rate and pump power. When the repetition rate was high (>70 kHz), the pulsed laser threshold gradually increased and output power decreased with the repetition rate. When operating at repetition rates below several tens of kilohertz, the laser delivered less than 10 ns pulses. The inset picture shows a typical oscilloscope trace of the laser pulses (~7 ns pulse width).

A single-mode Tm-doped fiber amplifier was used to boost output power of the single-frequency pulses. The amplifier was core pumped by another part (~70%) of the Er-doped fiber source through the use of single-mode fiber-pigtailed WDM for 1.55 μm/2 μm wavelengths. Heavily Tm-doped single-mode silicate fiber (7.8 μm fiber core, NA = 0.153, nonpolarization maintaining), made in-house, was used as the active fiber in the amplifier. Because of its high pump absorption and high laser gain, tens of centimeters long active fiber was sufficient to build the 2 μm fiber amplifier. Average output power

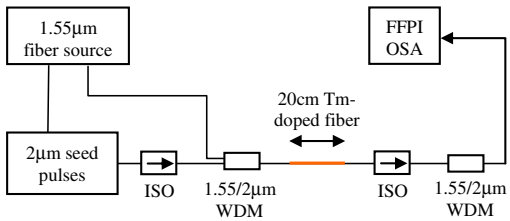

Fig. 1. (Color online) Schematic of a single-frequency pulsed Tm-doped fiber MOPA system: ISO, isolator; WDM, wavelength division multiplexing; FFPI, fiber Fabry–Perot interferometer; OSA, optical spectrum analyzer.

 © 2011 Optical Society of America

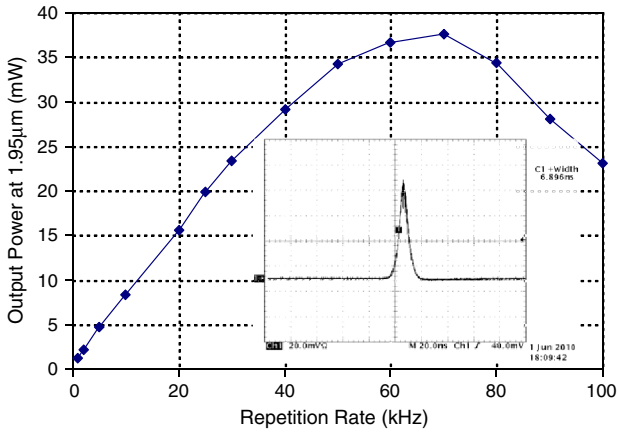

Fig. 2. (Color online) Average output power of the laser oscillator as a function of pulse repetition rate at a pump power of 300 mW. Inset, oscilloscope trace of typical laser pulses with a measured pulse width of 6.89 ns.

and corresponding peak power of the amplified laser pulses (as a function of total pump power at two repetition rates) are shown in Fig. 3, where the active fiber in the fiber amplifier had a length of 20 cm. The average power was measured with a power meter (Ophir-Spiricon, Model 3A) after the residual pump was dumped. Peak power was obtained from the measured average power and its corresponding pulse repetition rate and pulse width. Overall slope efficiency of the amplifier was about 64% at 50 kHz and 40% at 10 kHz repetition rates. Multikilowatt peak power was obtained at repetition rates of 10 kHz and below. We did not see significant difference in the pulse width and shape between the seed pulses and the amplified pulses. The inset picture in Fig. 3 shows a typical optical spectrum of the amplified pulses. A short length of active fiber used in the fiber amplifier allows suppressing many nonlinear effects in the active fiber. In addition, the short duration of the single-frequency pulses prevents the onset of SBS not only in the fiber amplifier but also in a long piece of passive fiber after the amplifier, as can be seen later.

The laser spectral linewidth was measured with an in-house fiber-based scanning Fabry–Perot interferometer, which was constructed with two identical high-reflective fiber Bragg gratings at the same wavelength as the laser

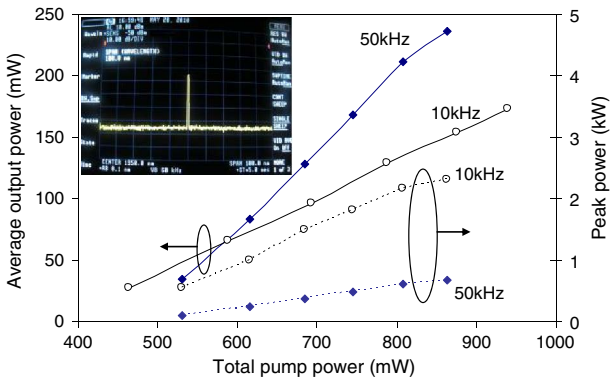

Fig. 3. (Color online) Average output power (solid curve) and its corresponding peak power (dotted curve) of the amplified laser pulses as a function of pump power. Inset, optical spectrum of the amplified pulses.

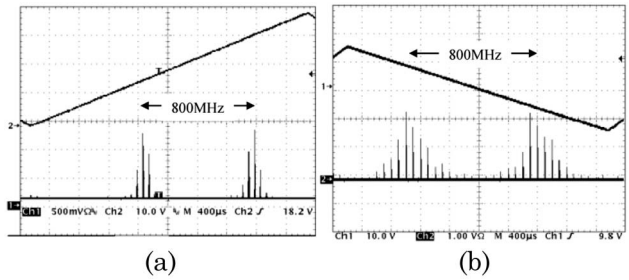

Fig. 4. Laser spectrum over one free spectral range (FSR = 800 MHz) of a Fabry–Perot interferometer, showing the spectral linewidth of (a) the single-frequency oscillator pulses and (b) after amplification. Spectral broadening of the amplified pulses is attributed to SPM in the long passive pigtail fiber after the fiber amplifier.

wavelength (1950 nm) as previously described [8]. Figure 4 shows typical scanning spectra (over one free spectral range, FSR = 800 MHz) of the laser pulses before and after amplification. The measured spectral width of the oscillator pulses was about $\Delta\nu \sim 50$ MHz. The pulse width was about $\Delta t \sim 6$–8 ns; thus, $\Delta\nu * \Delta t \sim$ 0.3–0.4, indicating single-frequency pulses from the oscillator are transform limited. For the amplified single-frequency pulses, however, the measured spectral linewidth ~150 MHz was significantly broadened (by a factor of 3). Because the laser pulse width was not reduced during pulse amplification, we attribute spectral broadening to a nonlinear effect in the fiber, such as SPM. Considering that the length of active fiber in the amplifier was only 20 cm, the observed nonlinear spectral broadening should be attributed to a long passive pigtail fiber of an isolator and a WDM located between the active fiber and the scanning fiber Fabry–Perot interferometer to prevent backreflection and for removal of the residual pump.

SPM-induced spectral broadening in the fiber can be estimated by the numerical value of the maximum nonlinear phase shift φ_{NL} [10], i.e., $\varphi_{\mathrm{NL}} = (2\pi/\lambda)n_2 \mathrm{LI}$, where n_2 is the nonlinear index coefficient, L is the fiber length, $I = P/(\pi r^2)$ is the laser intensity, P is the laser peak power, and r is the mode field radius. For silica glass fiber, $n_2 = 2.2 \times 10^{-20}\,\mathrm{m}^2/\mathrm{W}$ [10]. Given $L = 3$ m, $P = 1$ kW, $r = 5\,\mu$m, the nonlinear phase shift φ_{NL} can be calculated to be about 2.6. This indicates SPM results in spectral broadening by a factor of ~2.6 if 1 kW peak power 2 μm laser pulses propagate in 3 m long SMF-28 fiber, which is very similar to the case in the experiment. This SPM-induced spectral broadening can only be observed with the scanning Fabry–Perot interferometer but not an optical spectrum analyzer (OSA) due to its low resolution (see the inset in Fig. 3).

When those amplified laser pulses are coupled into a longer piece of silica fiber, other nonlinear effects can be observed. Figure 5 shows the spectra of the laser pulses when additional passive fiber was added. The sweep time of the OSA was much longer than the period of the repetitive pulses. Therefore, the OSA spectra in Fig. 5 were actually an averaged spectrum of many laser pulses. As compared with the inset picture in Fig. 3, the laser spectra have been significantly broadened. The added fiber was Corning SMF-28 fiber. At the wavelength near 2 μm, the fiber exhibits strong anomalous group-velocity

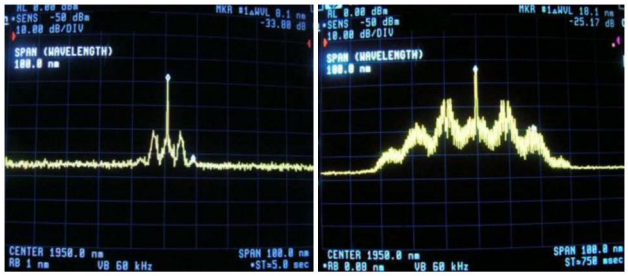

(a) (b)

Fig. 5. (Color online) Optical spectra of laser pulses after propagation in a long piece of Corning SMF-28 fiber: (a) ~300 W peak power pulses in a 75 m fiber and (b) ~1 kW peak power pulses in a 5 m fiber.

dispersion (GVD). The spectral broadening can be attributed to MI, which is evidenced by the well-known characteristic MI sidebands [10]. Up to two to three sets of MI gain peaks can be seen in the spectrum. Our measurements showed that pulses at MI sidebands had significantly shorter pulse widths (<1 ns) than the main pulses. Although the main pulses were highly stable, amplitudes of MI-induced pulses at the sidebands were highly fluctuated. These experimental results indicate that the nanosecond pulses have been broken down to form higher peak power shorter pulses by MI during their propagation in the long piece of fiber, which paves the way to generate the mid- and long-IR supercontinuum [7].

The sidebands in Fig. 5 can be explained theoretically. When the pump wavelength lies in the anomalous GVD regime and deviates considerably from a zero dispersion wavelength (1.3 μm for SMF-28 fiber), which is the case in our experiment, phase-matching conditions can still be achieved in some wavelength regions by SPM in the fiber by generating sidebands located at $\omega_o + / - \Delta\omega$. The sideband frequency shift is given by $\Delta\omega = (2\gamma P_o/|\beta_2|)1/2$, where γ is the nonlinearity coefficient, P_o is the peak power of the pump, and β_2 is the GVD parameter of the fiber at the pump wavelength [10].

From the sidebands of the laser spectra in Fig. 5, we can calculate the corresponding laser peak powers. For Corning SMF-28 fiber, $\gamma = 2\pi n_2/\lambda(\pi r^2) \sim 0.9\, W^{-1}\mathrm{km}^{-1}$. The GVD, β_2, of the fiber at 1.95 μm is about ~60 ps/km.nm or −121 ps^2/km. The wavelength shifts of the first-order MI sideband peaks in Fig. 5 are 4 nm and 9 nm, corresponding to frequency shifts (calculated by $\Delta\nu = \Delta\omega/2\pi$) of 0.32 THz and 0.71 THz, respectively. Thus, peak powers of the laser pulses in the spectra of Fig. 5 can be calculated to be 0.26 and 1.32 kW, which are consistent with the experiment.

In summary, kilowatt-peak-power single-frequency pulses have been demonstrated in a Tm-doped fiber master oscillator power amplifier (MOPA) system. A short length of active fiber in the fiber amplifier and a short pulse duration enable generation of high-peak-power pulses without an onset of SBS. The transform-limited single-frequency pulses experienced slight spectral broadening due to SPM in passive pigtail fibers of the components in the fiber amplifier. After propagation in longer passive fiber, these high-peak-power pulses can be broken down to form higher peak power solitons by MI, which paves the way to generate the mid- and long-IR supercontinuum.

We acknowledge financial support from the United States Air Force and the National Aeronautics and Space Administration (NASA). The authors would also like to acknowledge technical support from Doctor Farzin Amzajerdian of the NASA Langley Research Center and the valuable comments from Doctor Kenneth L. Schepler of the Air Force Research Lab.

References

1. S. W. Henderson, P. J. M. Suni, C. P. Hale, S. M. Hannon, J. R. Magee, D. L. Bruns, and E. H. Yuen, IEEE Trans. Geosci. Remote Sensing **31**, 4 (1993).
2. J. Yu, U. N. Singh, N. P. Barnes, and M. Petros, Opt. Lett. **23**, 780 (1998).
3. G. J. Koch, M. Petros, J. Yu, and U. N. Singh, Appl. Opt. **41**, 1718 (2002).
4. J. Yu, B. C. Trieu, E. A. Modlin, U. N. Singh, M. J. Kavaya, S. Chen, Y. Bai, P. J. Petzar, and M. Petros, Opt. Lett. **31**, 462 (2006).
5. S. Chandra, M. E. Wager, B. Clayton, A. G. Geiser, T. H. Allik, J. L. Ahl, C. R. Miller, P. A. Budni, P. A. Ketteridge, K. G. Lanier, E. P. Chicklis, J. A. Hutchinson, and W. W. Hovis, Proc. SPIE **4036**, 200 (2000).
6. M. Schellhorn, M. Eichhorn, C. Kieleck, and A. Hirth, C.R. Phys. **8**, 1151 (2007).
7. C. Xia, M. Kumar, O. P. Kulkarni, M. N. Islam, F. L. Terry, Jr., M. J. Freeman, M. Poulain, and G. Maźe, Opt. Lett. **31**, 2553 (2006).
8. J. Geng, Q. Wang, T. Luo, F. Amzajerdian, and S. Jiang, Opt. Lett. **34**, 3713 (2009).
9. M. Leigh, W. Shi, J. Zong, Z. Yao, S. Jiang, and N. Peyghambarian, Appl. Phys. Lett. **92**, 181108 (2008).
10. Govind P. Agrawal, *Nonlinear Fiber Optics*, 3rd ed. (Academic, 2001).